RSC Advances

Table of Contents

POP-Sulfur composite as cathode material for Lithium-Sulfur battery.

COMMUNICATION

Improved Cyclability of Lithium-Sulfur Battery with POP-Sulfur Composite Materials

Wei Weng,[a] Shengwen Yuan,[a] Nasim Azimi,[a,d] Zhang Jiang,[b] Yuzi Liu,[c] Yang Ren,[c] Ali Abouimrane,[a] and Zhengcheng Zhang[a*]

The microporous nature of the porous organic polymer (POP) successfully limits the crystallization of sulfur and hence restrains the dissolution and diffusion of lithium polysulfides formed during the repeated charge and discharge process of lithium-sulfur battery. In this study, we demonstrated for the first time that POP-Sulfur nanocomposite can afford high coulombic efficiency and superior reversibility in lithium-sulfur battery.

Lithium batteries are one of the most promising energy sources to power the next-generation electric vehicles.[1,2] The energy density requirement for a 40-mile all-electric range in a plug-in hybrid electric vehicle (PHEV) is 3~5 times more than the achievable by current lithium-ion technology.[3] Thus, development of new, emerging electrode materials with higher energy density is urgently needed for lithium ion battery. Alternatively, rechargeable batteries beyond lithium-ion have been widely investigated.[4] Among them, lithium-sulfur (Li-S) battery is a promising chemistry for a number of desirable properties. Sulfur has high capacity (1675 mAg^{-1} based on the electrochemical reaction of $16Li + S_8 \rightarrow 8Li_2S$) and specific energy density (2500 Whkg^{-1}); Sulfur is naturally abundant, environmentally benign and less expensive. Despite the great promise, there are still a number of challenges to be addressed before the practical application, including significant capacity fading during charge-discharge cycling, low coulombic efficiency (CE), insufficient cycle life, and high self-discharge rate.[5-9]

During the discharge of Li-S battery, a series of lithium polysulfide intermediates (Li_2S_x, x=1-8) are generated. High order lithium polysulfides (4<x<8) are generated in the initial discharge stage, which are soluble in the electrolyte and the final discharge products Li_2S or Li_2S_2 are low order polysulfides and tend to precipitate on the surface of the electrode and become unusable. Both the dissolution of polysulfides and the generation of resistive Li_2S/Li_2S_2 lead to the loss of active sulfur material causing fast capacity fade upon cycling.[10] During the charge, the dissolved lithium polysulfides are reduced to low order polysulfides on the lithium anode, which then diffuses back to the sulfur cathode and gets oxidized, causing a so-called "redox shuttling" phenomenon significantly lowering the

columbic efficiency. Accordingly, many studies have been conducted to solve the issues associated with this battery chemistry. There are reports on Li-S battery using coated current collector,[11] coated porous separator for enhanced electrochemical performance of Li-S battery,[12] and new electrolyte to improve performance of Li-S battery.[13] Most research are aimed at maintaining the mechanical and electrical integrity of the sulfur electrode by embedding lithium polysulfides within the framework of a substrate, such a substrate could be mesoporous carbon,[14-17] carbon nanotube,[18-20] carbon nanofiber,[21] carbon sphere,[22] graphene,[23-25] graphene oxide[26-28] and conductive polymer.[29-32] Although great improvement has been achieved, the synthesis of such materials with controlled size and the uniform distribution of the pores poses a great challenge.[33] In this communication, we report a new sulfur electrode embedded in an easily available porous organic polymer (POP) network.

POPs represent a new class of amorphous polymeric materials with tuneable permanent porosity.[34-36] The polymer networks possess large Brunauer-Emmett-Teller (BET) surface area comparable to that of crystalline inorganic microporous materials, such as zeolites, silicas, activated carbon, and metal-organic frameworks. POPs are constructed exclusively by strong covalent bonds of rigid backbone (struts) and aromatic building blocks (nodes). The high rigidity of the materials is crucial for the mitigation of the chain flexibility, which can reduce the fluctuation of pore size and render the pore structure substantially more stable. The pore geometry and pore size distribution can be controlled by careful selection of 3D-directing "nodes" with "struts" of different lengths. Due to their unique physicochemical property, POPs have found many applications in gas storage, separation, and catalysis. However, little research has been conducted in the electrochemical energy storage system. It is our original idea to investigate the high surface area POP as a substrate to host active sulfur material for Li-S battery. The non-polar groups in the POP have strong interaction with the non-polar sulfur and the conductive additive. POP substrate is expected to restrain the sulfur and the Li_2S_x and prevent the dissolution and subsequent diffusion of Li_2S_x species into the electrolyte thus enhancing the reversibility of the Li-S battery.
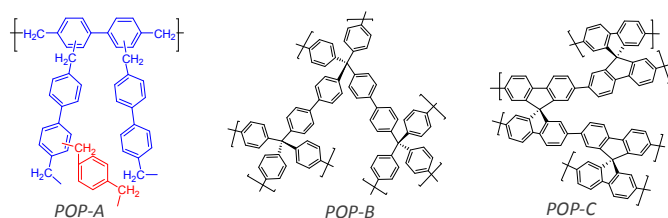
Fig. 1 Chemical structure of POP-A, POP-B, and POP-C.

In this communication, we report the improved cyclability of a Li-S battery using POP-Sulfur composite material. Fig. 1 showed the chemical structure of three polymers, POP-A, POP-B and POP-C, which can be readily prepared following the previously reported procedure of a one-step polymerization reaction with suitable monomers.[37-38] The detailed synthesis of these POPs are described in Supplementary Information. The BET surface area of the porous carbon materials used for Sulfur-Carbon composite[14-22] is usually less than 1000 m^2g^{-1}. In contrast, POPs in this study have much higher surface area (up to 3143 m^2g^{-1}) than the porous carbon materials. Moreover, these POPs exhibit dominant micropores with pore size less than 1 nm as calculated from the Non-Local Density Functional Theory (NLDFT) (Fig. S1 in Supplementary Information). The highly strained tetrahedral monomer in POP-B and POP-C cross-links with three or four other monomers to extend the network three dimensionally thus enables the formation of a robust network with less penetration and high surface area.

Fig. 2a and 2b show 1D Wide-angle X-ray scattering (WAXS) pattern and the pore size distribution of the POPs fitted to the Percus-Yevick hard-sphere approximation.[39-41] Fig. 2c gives the comparison of the pore size measured by the X-ray technique and calculated by NLDFT method. The difference is probably caused by the ideal sphere model used for pore shapes, which ignores the irregular cross-linked molecular architecture. Both X-ray and NLDFT data, however, are qualitatively consistent with each other: POP-B has the largest pore size and POP-A has the smallest pore size.
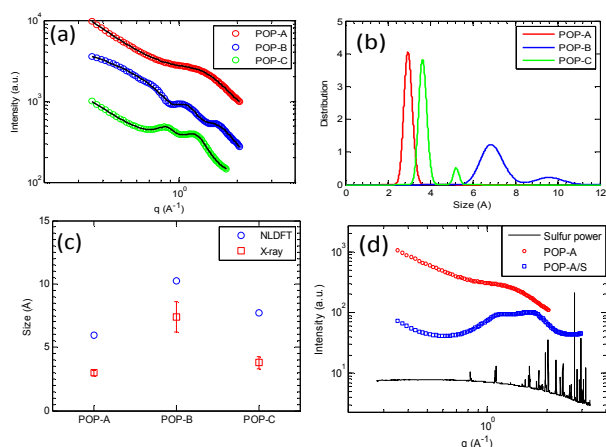

Fig. 2 1D WAXS data from POP samples (a), normalized pore size distributions from the best fitting (b), comparison of pore sizes from WAXS and NLDFT (Mean size and size of largest distribution were used for WAXS and NLDFT, respectively) (c), and XRD pattern of sulfur powder and WAXS profiles of POP-A and POP-A-S composite (d). (Curves in (a) and (d) are shifted vertically for clarity.)

POP-Sulfur composites were prepared by the thermal treatment of the mixture of sulfur and POPs after homogenization by a ball milling process as illustrated in Fig. 3. The melting-down process afforded micro-size agglomerates of POP and sulfur composites in all three samples as observed by SEM (Fig. S2 in Supplementary Information). Transmission electron microscopy (TEM) of the POP-A-Sulfur composite is shown in Fig. 4a and 4b. No diffraction contrast from grains was observed in the POP-A-Sulfur images confirming that sulfur particles are well dispersed in the POP matrix. This is in good agreement with the results from WAXS experiment and no sharp diffraction peaks of crystalline sulfur was observed for POP-A-Sulfur composite (Fig. 2d). The elemental mapping by energy-filtered TEM further confirms a homogeneous distribution of sulfur in the porous polymer even at the nanoscale, as shown in Fig. 4c-4e.
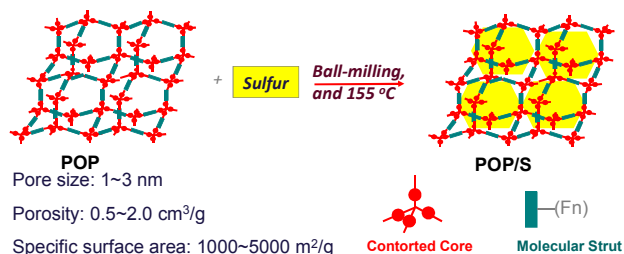

Fig. 3 Preparation of POP-Sulfur composites with micropores as host materials for accommodation of nanosized sulfur particles.
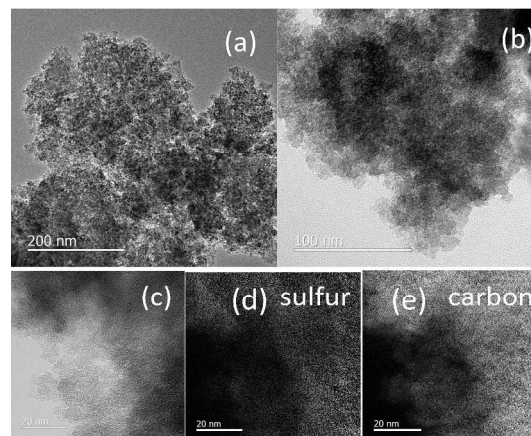

Fig. 4 TEM images of POP-A-S composite (a) and (b), TEM image (c) and corresponding EDX elemental mappings of POP-A-S composite for sulfur (d) and carbon (e).

Another evidence of the incorporation of sulfur into the micropores of POPs is the significant reduction of the BET surface area after the ball milling and thermal treatment. The surface area of POP-A is reduced from 1362 m^2g^{-1} to 104 m^2g^{-1} when the composite (1:1 by weight) is formed and this reduction is more drastic for POP-B and POP-C. Additionally, the total pore volume of POPs also decreases dramatically after encapsulation with sulfur (in cm^3g^{-1}, POP-A: 1.292; POP-A-Sulfur: 0.20; POP-B: 2.07; POP-B-Sulfur: 0.09; POP-C: 0.94; POP-C-Sulfur: 0.05), suggesting that sulfur is infused into the POP pores.

The charge/discharge voltage profiles of Li-S cells containing POP-Sulfur composite are presented in Fig. 5. Fig. 5a shows the first charge and discharge voltage profiles for POP-A-Sulfur cell. The

discharge capacity is 927 mAhg[-1] at a current density of 200 mAg[-1] and the subsequent charge capacity is 898 mAhg[-1], corresponding to a high coulombic efficiency of 97 %. As shown in Fig. 5b, the high coulombic efficiency for POP-A-Sulfur cell is maintained even after 100 cycles, suggesting the successful restraint of polysulfide dissolution and the redox shuttling effect. Such a high coulombic efficiency in the whole cycle range for a sulfur cathode is quite rare.[42] Wang *et al.*[43] reported a PAN/Sulfur composite cathode maintained a capacity of 600 mAhg[-1] after 50 cycles. More recently, a PAN nanotube/Sulfur cathode by Liu *et al.*[29] was reported to deliver a capacity of 837 mAhg[-1] after 100 cycles at low rate. However, for both composite cathodes, a long activation process (~ 20 cycles) is required to reach the maximum discharge capacity, and the shuttle mechanism still exists. The excellent performance of POP-A-Sulfur composite clearly indicates that the highly porous structure and high hydrophobic nature of the POPs significantly suppresses the dissolution of polysulides and enables a highly reversible Li-S battery.

Li-S cell testing data for POP-B-Sulfur and POP-C-Sulfur composites are shown in Fig. 5c and 5d. It is notable that the charge and discharge voltage profiles of POP-Sulfur composites showed different potential polarization, which might be caused by the different porous structure and the pore volume reduction after the sulfur infusion. As shown in Fig. 5d, both POP-B and POP-C composite cells can achieve high coulombic efficiency in the initial cycle and the values are slightly greater than 100 % in the following cycles, indicating that the shuttle mechanism was completely suppressed in the POP-B and POP-C systems. The reversibility of the three POP-Sulfur composites is impressive given the absence of the widely reported efficient additives such as $LiNO_3$,[44] P_2S_5,[45] fluorinated ether[13] or lithium polysulfide dissolved in the electrolyte as electro-active catholyte.[46,47]

In conclusion, the porous organic polymer with microporous structure and large surface area has been demonstrated for the first time as an effective substrate to accommodate sulfur active materials and suppress the lithium polysulfides dissolution. The POP-Sulfur nanocomposite electrodes showed excellent reversibility in Li-S cell. This research provides an insight that POPs play a vital role in addressing the technical barriers for the lithium-sulfur chemistry. However, for the practical use in electric vehicles, the high practical energy density for Li-S battery is extremely desired. For the future work, POPs could be replaced by a conductive polymer with unique microporous structure such as conjugated microporous polymers (CMPs) that combine π-conjugated skeletons with permanent nanopores with the hope to eliminate or reduce the amount of conducting agent in the sulfur electrode to greatly improve the practical energy density of Li-S battery.[46]

Acknowledgments

Notes and references

a Chemical Sciences and Engineering Division, Argonne National Laboratory, Argonne, IL 60439, USA

b Advanced Photon Source, Argonne National Laboratory, Argonne, IL 60439, USA

c Center for Nanoscale Materials, Argonne National Laboratory, Argonne, IL 60439, USA

d Departments of Chemical Engineering and Bioengineering, University of Illinois at Chicago, Chicago, IL 60607, USA

Chemical Sciences and Engineering Division, Argonne National Laboratory, 9700 South Cass Avenue, Argonne, IL 60439-4837, USA
Fax: 1-630-972-4440; Tel: 1-630-252-5258; E-mail: weng@anl.gov
Fax: 1-630-972-4440; Tel: 1-630-252-7506; E-mail: syuan@anl.gov
Fax: 1-630-972-4440; Tel: 1-630-252-5486; E-mail: nzazimi@anl.gov
Tel: 1-630-252-3118; E-mail: zjiang@aps.anl.gov
Tel: 1-630-252-1775; E-mail: yuziliu@anl.gov
Tel: 1-630-252-0363; E-mail: ren@aps.anl.gov
Tel: 1-630-252-3729; E-mail: abouimrane@anl.gov
Fax: 1-630-972-4440; Tel: 1-630-252-7868; E-mail: zzhang@anl.gov

Author Information

Corresponding Author

*e-mail: zzhang@anl.gov

Author Contributions

W.W. and S.Y. contributed equally to this work.

†Electronic Supplementary Information (ESI) available: [Experimental procedure, illustration of coin cell assembly with different prelithiation techniques]. See DOI: 10.1039/c000000x/
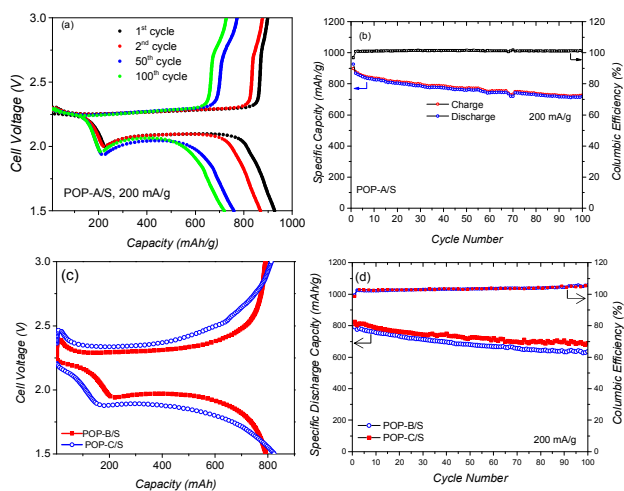

Fig. 5 Li-S cells with POP-Sulfur composite cathodes cycled between 1.5 and 3.0 V at a current density of 200 mAg[-1] current. Voltage profiles (a), and capacity retention (b) of POP-A-S composite cell; 1st cycle charge discharge profiles of POP-B-S and POP-C-S composite cells (c), and cycling performance of POP-B-S and POP-C-S composite cells (d). (Electrolyte: 1M LiTFSI in 1,3-dioxolane (DOL) and $CHF_2CF_2CH_2OCF_2CF_2H$ in a 1:2 volume ratio.)

1   M. M. Thackeray, C. Wolverton and E. D. Isaacs, *Energy Environ. Sci.,* 2012, **5**, 7854.

2   M. Armand and J. M. Tarascon, *Nature,* 2008, **451**, 652.

3   V. Etacheri, R. Marom, R. Elazari, G. Salitra and D. Aurbach, *Energy Environ. Sci.,* 2011, **4**, 3243.

4   (a) Z. Peng, S. A. Freunberger, Y. Chen and P. G. Bruce, *Science,* 2012, **337**, 563; H.-G. Jung, J. Hassoun, J.-B. Park, Y.-K. Sun and B. Scrosati, *Nat. Chem.,* 2012, **4**, 579; (b) J. Muldoon, C. B. Bucur, A. G. Oliver, T. Sugimoto, M. Matsui, H. S. Kim, G. D. Allred, J. Zajicek and Y. Kotani, *Energy Environ. Sci.,* 2012, **5**, 5941; T. Zhang, Z. Tao and J. Chen, *Mater. Horiz.,* 2014, DOI: 10.1039A.

5   H. Yamin and E. Peled, *J. Power Sources,* 1983, **9**, 281.

6   Y. Fu and A. Manthiram, *RSC Adv.*, 2012, **2**, 5927.

7   X. L. Ji, K. T. Lee and L. F. Nazar, *Nat. Mater.,* 2009, **8**, 500.

8   J. Shim, K. A. Striebel and E. J. Cairns, *J. Electrochem. Soc.,* 2002, **149**, A1321.

9   H. Yamin, A. Gorenshtein, J. Penciner, Y. Sternberg and E. Peled, *J. Electrochem. Soc.,* 1988, **135**, 1045.

10   K. Kumaresan, Y. Mikhaylik and R. E. White, *J. Electrochem. Soc.,* 2008, **155**, A576.

11   L. Wang, X. He, J. Li, J. Gao, M. Fang, G. Tian, J. Wang and S. Fan, *J. Power Sources*, 2013, **239**, 623.

12   Z. Zhang, Y. Lai, Z. Zhang, K. Zhang and J. Li, *Electrochim. Acta*, 2014, **129**, 55.

13   N. Azimi, W. Weng, C. Takoudis and Z. Zhang, *Electrochem. Commun.*, 2013, **37**, 96.

14   X. L. Li, Y. L. Cao, W. Qi, L. V. Saraf, J. Xiao, Z. M. Nie, J. Mietek, J. G. Zhang, B. Schwenzer and J. Liu, *J. Mater. Chem.,* 2011, **21**, 16603.

15   J. Schuster, G. He, B. Mandlmeier, T. Yim, K. T. Lee, T. Bein and L. F. Nazar, *Angew. Chem., Int. Ed.,* 2012, **51**, 3591.

16   S. R. Chen, Y. P. Zhai, G. L. Xu, Y. X. Jiang, D. Y. Zhao, J. T. Li, L. Huang and S. G. Sun, *Electrochim. Acta,* 2011, **56**, 9549.

17   Y. Yang, G. H. Yu, J. J. Cha, H. Wu, M. Vosgueritchian, Y. Yao, Z. A. Bao and Y. Cui, *ACS Nano* 2011, **5**, 9187.

18   S. Dorfler, M. Hagen, H. Althues, J. Tubke, S. Kaskel, M. J. Hoffmann, *Chem. Commun.,* 2012, **48**, 4097.

19   J. C. Guo, Y. H. Xu and C. S. Wang, *Nano Lett.*, 2011, **11**, 4288.

20   S. S. Jeong, Y. Lim, Y. J. Choi, G. B. Cho, K. W. Kim, H. J. Ahn and K. K. Cho, *J. Power Sources,* 2007, **174**, 745.

21   L. Ji, M. Rao, S. Aloni, L. Wang, E. J. Cairns and Y. Zhang, *Energy Environ. Sci.,* 2011, **4**, 5053.

22   B. Zhang, X. Qin, G. R. Li and X. P. Gao, *Energy Environ. Sci.,* 2010, **3**, 1531.

23   H. L. Wang, Y. Yang, Y. Y. Liang, J. T. Robinson, Y. G. Li, A. Jackson, Y. Cui and H. J. Dai, *Nano Lett.,* 2011, **11**, 2644.

24   J. Z. Wang, L. Lu, M. Choucair, J. A. Stride, X. Xu and H. K. Liu*, J. Power Sources,* 2011, **196**, 7030.

25   N. W. Li, M. B. Zheng, H. L. Lu, Z. B. Hu, C. F. Shen, X. F. Chang, G. B. Ji, J. M. Cao and Y. Shi, *Chem. Commun.,* 2012, **48**, 4106.

26   F. F. Zhang, X. B. Zhang, Y. H. Dong and L. M. Wang, *J. Mater. Chem.,* 2012, **22**, 11452.

27   L. W. Ji, M. M. Rao, H. M. Zheng, L. Zhang, Y. C. Li, W. H. Duan, J. H. Guo, E. J. Cairns and Y. G. Zhang, *J. Am. Chem. Soc.* 2011, **133**, 18522.

28   L. Zhang, L. Ji, P.-A. Glans, Y. Zhang, J. Zhu and J. Guo, *Phys. Chem. Chem. Phys.,* 2012, **14**, 13670.

29   L. F. Xiao, Y. L. Cao, J. Xiao, B. Schwenzer, M. H. Engelhard, L. V. Saraf, Z. M. Nie, G. J. Exarhos and J. Liu, *Adv. Mater.,* 2012, **24**, 1176.

30   F. Wu, J. Z. Chen, R. J. Chen, S. X. Wu, L. Li, S. Chen and T. Zhao, *J. Phys. Chem. C,* 2011, **115**, 6057.

31   F. Wu, S. X. Wu, R. J. Chen, J. Z. Chen and S. Chen, *Electrochem. Solid-State Lett.,* 2010, **13**, A29.

32   J. Wang, J. Chen, K. Konstantinov, L. Zhao, S. H. Ng, G. X. Wang, Z. P. Guo and H. K. Liu, *Electrochim. Acta,* 2006, **51**, 4634.

33   J. Lee, J. Kim and T. Hyeon, *Adv. Mater.,* 2006, **18**, 2073.

34   P. Kaur, J. T. Hupp and S. T. Nguyen, *ACS Catal.,* 2011, **1**, 819.

35   Y. Zhang and S. N. Riduan, *Chem. Soc. Rev.,* 2012, **41**, 2083.

36   N. B. McKeown and P. M. Budd, *Chem. Soc. Rev.,* 2006, **35**, 675.

37   C. D. Wood, B. Tan, A. Trewin, H. Niu, D. Bradshaw, M. J. Rosseinsky, Y. Z. Khimyak, N. L. Campbell, R. Kirk, E. Stöckel and A. I. Cooper, *Chem. Mater.,* 2007, **19**, 2034.

38   S. Yuan, B. Dorney, D. White, S. Kirklin, P. Zapol, L. Yu and D.-J. Liu, *Chem. Commun.,* 2010, **46**, 4547.

39   D. J. Kinning and E. L. Thomas, *Macromolecules,* 1984, **17**, 1712.

40   J. J. Pedersen, *Appl. Crystallogr.,* 1994, **27**, 595.

41   T. Sun, S. Donthu, M. Sprung, K. D'Aquila, Z. Jiang, A. Srivastava, J. Wang and V. P. Dravid, *Acta Mater.,* 2009, **57**, 1095.

42   W. Weng, V. G. Pol and K. Amine, *Adv. Mater.,* 2013, **25**, 1608.

43   J. Wang, J. Yang, J. Xie and N. Xu, *Adv. Mater.,* 2002, **14**, 963.

44   D. Aurbach, E. Pollak, R. Elazari, G. Salitra, C. S. Kelley and J. J. Affinito, *J. Electrochem. Soc.,* 2009, **156**, A694.

45   Z. Lin, Z. Liu, W. Fu, N. J. Dudney and C. Liang, *Adv. Funct. Mater.,* 2013, **23**, 1064.

46   R. Xu, I. Belharouak, J. C. M. Li, X. Zhang, I. Bloom and J. Bareño, *Adv. Energy Mater.,* 2013, **3**, 833.

47   S. Chen, F. Dai, M. L. Gordin and D. Wang, *RSC Adv.,* 2013, **3**, 3540.

48   Y. Xu, S. Jin, H. Xu, A. Nagai and D. Jiang, *Chem. Soc. Rev.*, 2013, **42**, 8012.